

RESEARCH ARTICLE OPEN ACCESS

# Decrease in Effective Population Size After the Immigration of Asian Black Bears to Japan

Naoki Ohnishi<sup>1</sup>  | Valentin Guskov<sup>2</sup> | Shuri Kato<sup>3</sup> | Ririko Koido<sup>4</sup> | Kentaro Uchiyama<sup>5</sup> | Yoshiaki Tsuda<sup>6</sup>

<sup>1</sup>Tohoku Research Center, Forestry and Forest Products Research Institute, Morioka, Japan | <sup>2</sup>Federal Scientific Center of the East Asia Terrestrial Biodiversity Far Eastern Branch of the Russian Academy of Sciences, Vladivostok, Russia | <sup>3</sup>Tama Forest Science Garden, Forestry and Forest Products Research Institute, Tokyo, Japan | <sup>4</sup>Graduate School of Science and Technology, University of Tsukuba, Ibaraki, Japan | <sup>5</sup>Department of Forest Molecular Genetics and Biotechnology, Forestry and Forest Products Research Institute, Ibaraki, Japan | <sup>6</sup>Sugadaira Research Station, Mountain Science Center, University of Tsukuba, Ueda, Japan

**Correspondence:** Naoki Ohnishi ([ohnishi\\_naoki320@ffpri.go.jp](mailto:ohnishi_naoki320@ffpri.go.jp)) | Yoshiaki Tsuda ([tsuda.yoshiaki.ge@u.tsukuba.ac.jp](mailto:tsuda.yoshiaki.ge@u.tsukuba.ac.jp))

**Received:** 14 July 2025 | **Revised:** 10 December 2025 | **Accepted:** 11 December 2025

**Keywords:** ddRADseq | genetic structure | population size | reduced representation genome sequencing | *Ursus thibetanus*

## ABSTRACT

The genetic structure and demographic history of the Asian black bear (*Ursus thibetanus*) in Japan were investigated using Double digest restriction-site associated DNA sequencing (ddRADseq). Analysis of 83 individuals revealed seven regional populations with clear geographic structure. Bayesian clustering and principal coordinate analysis showed low genetic differentiation in central populations and higher divergence in peripheral populations. The fluctuation of effective population size ( $N_e$ ) inferred from SNP data showed an initial decline until around 200,000 years ago, followed by two additional reductions in most populations, with no evidence of recovery. These declines likely correspond to migration from the continent, habitat loss during the Last Glacial Maximum, and human expansion. Nuclear data suggest male-biased gene flow across mitochondrial DNA lineage boundaries. Isolated populations exhibited low heterozygosity and high genetic differentiation, emphasizing the impact of habitat fragmentation. This is the first large-scale population genomic study of Asian black bears and provides important insights for conservation and future genomic research.

## 1 | Introduction

Genetic diversity, which is the result of long-term evolutionary processes, forms the foundation for the survival, adaptation, and development of species (Meffe and Carroll 1997). While it is relatively easy to infer current population structures from genetic data, identifying the true population formation processes from among various potential alternative scenarios remains challenging. Population genomic research can complement phylogeographic insights based on mitochondrial DNA (mtDNA) (Edwards and Bensch 2009; Toews and Brelsford 2012; Cronin 1993) and provide new insights into

how species have diverged over time across different geographic ranges. Understanding the genetic population structure and evolutionary history of a species is therefore essential for guiding conservation and reintroduction strategies (Groom et al. 2006).

Analyses of genetic structure in species with broad geographic distributions have greatly enhanced our understanding of the factors shaping the composition of fauna across vast regions (De Kort et al. 2021). The field of population genomics is playing an increasingly important role in clarifying both natural and anthropogenic influences on the evolutionary trajectories of

Naoki Ohnishi, Valentin Guskov, and Yoshiaki Tsuda contributed equally as first and corresponding authors, respectively.

This is an open access article under the terms of the [Creative Commons Attribution](#) License, which permits use, distribution and reproduction in any medium, provided the original work is properly cited.

© 2026 The Author(s). *Ecological Research* published by John Wiley & Sons Australia, Ltd on behalf of The Ecological Society of Japan.

widely distributed species. Furthermore, it has become an indispensable tool for the development of effective conservation and management strategies (Hohenlohe et al. 2021).

The Asian black bear (*Ursus thibetanus*) is widely distributed throughout Asia, adapted to broadleaf forests, and plays an important ecological role in natural environments. It comprises seven extant subspecies, including the Japanese black bear (*U. t. japonicus*), and is considered the most phylogenetically ancient among the five East Asian subspecies, having diverged approximately 1.48 to 1.0 million years ago (Wu et al. 2015). It was previously believed that the Asian black bear migrated to the Japanese Archipelago only once during the Middle Pleistocene, around 600,000 to 400,000 years ago (Kawamura 2000; Ohnishi et al. 2009). Subsequently, mtDNA analyses have revealed that the bear populations within Japan diverged into three distinct lineages separated by Lake Biwa (Figure 1, Ohnishi et al. 2009). These three lineages are estimated to have diverged between 100,000 and 500,000 years ago, with minimal gene flow among regions thereafter (Ohnishi et al. 2009; Wu et al. 2015). However, recent whole genome sequencing (WGS) analysis using two individuals—one from the eastern cluster, captured near the SAL population examined in this study, and one from the southern cluster, representing an individual from Shikoku Island, with both belonging to different mtDNA clusters—showed a small genetic distance between the two and suggested that population structure occurred approximately 30,000 years ago (Kishida

et al. 2022). This is likely due to sex-biased dispersal capacity. In many mammalian species, postnatal dispersal tends to be male-biased, and the Asian black bear is no exception. A study of populations in the eastern cluster reported an average dispersal distance of  $4.8 \pm 1.7$  km (median 2.2 km) for females and  $17.4 \pm 3.5$  km (median 11.7 km) for males (Takayama et al. 2023). Moreover, in populations east of Lake Biwa, male-biased sex ratios were observed at the periphery of haplotypes with region-specific distributions (Ohnishi and Osawa 2014). Such male-biased dispersal likely maintained nuclear gene flow even after the population structuring around 30,000 years ago (Kishida et al. 2022).

Given the difference in resolution between analyses based on sequences of approximately 700 bp and WGS based on 2.20 Gbp, the simpler conclusions drawn by Ohnishi et al. (2009) need to be re-evaluated. However, the previous study was based on only two individuals sampled from two localities (Kishida et al. 2022), underscoring the need for genomic analysis using multiple samples from various regions.

The present study aims to re-examine the population formation history of the Asian black bear populations in Japan. To this end, we collected multiple individuals from multiple regions and applied a reduced-representation genome sequencing method (ddRADseq) to elucidate their genetic structure and to estimate historical changes in effective population size.

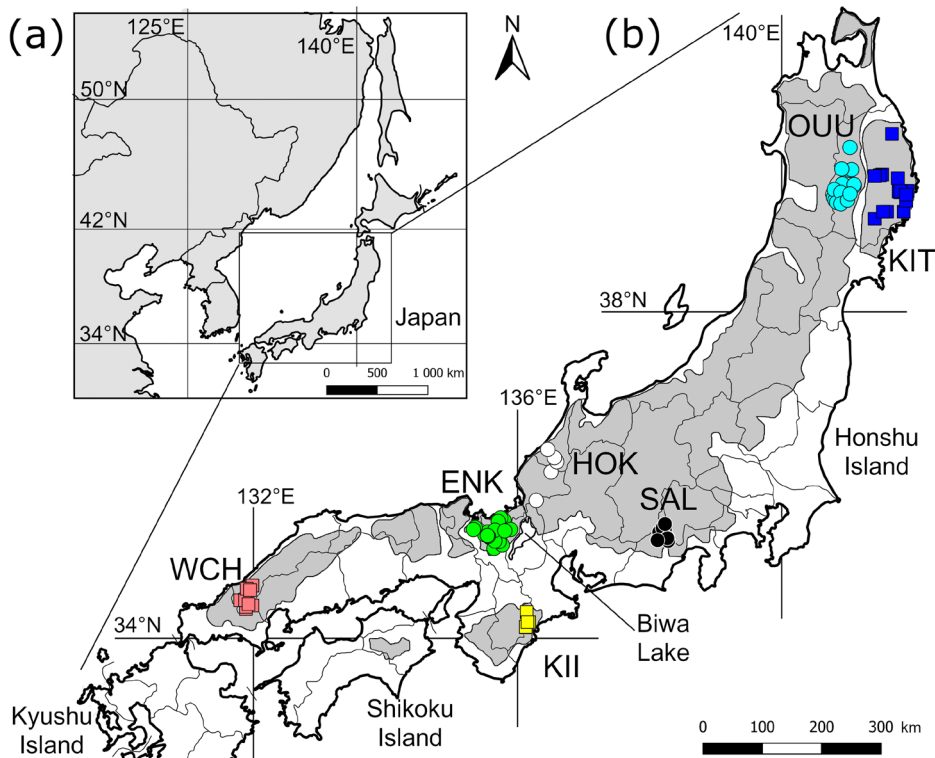


**FIGURE 1** | Study area and sampling locations. (a) A map of the major Japanese islands and the Far East of the Asian continent. (b) Distribution of the Asian black bear in Japan (shaded in gray) and capture locations of the samples used in this study. The symbols for capture locations correspond to those used in Figures 3 and 4, and the abbreviations of local populations are labeled next to each symbol. The following population names and abbreviations are used: Kitakami Mountains (KIT), Ouu Mountains (OUU), Southern Alps (SAL), Hokuriku (HOK), Eastern–Northern Kinki (ENK), Kii Peninsula (KII), and Western Chugoku (WCH). The two black stars indicate the capture sites of the two individuals analyzed by Kishida et al. (2022).

## 2 | Materials and Methods

### 2.1 | DNA Extraction and Sequencing

Muscle tissue samples from 85 Asian black bears inhabiting the largest island of Japan were collected (Figure 1, Table S1). These individuals were captured between 1998 and 2008 as part of nuisance control operations. Genomic DNA was extracted from each tissue sample using the MagExtractor (TOYOB0), and double digest restriction-site associated DNA sequencing (RAD-seq) was conducted following a protocol that combines the standard method of Peterson et al. (2012) with the amplicon tagging protocol for Access Array technology (Fluidigm, South San Francisco, CA, USA).

Genomic DNA was digested with two types of restriction enzymes, and Y-shaped adapters were ligated to the resulting fragments. PCR amplification was performed using adapter-specific primers with barcodes (Access Array Barcode Library for Illumina, Fluidigm) to enable sample identification. Equal amounts of amplified DNA from each sample were pooled and size-selected using BluePippin agarose gel cassettes (Sage Science, Beverly, MA, USA) to construct the RAD-seq libraries. The enzyme pairs used were SbfI-MseI and SphI-EcoRI, and 450 bp fragments were selected. The libraries were sequenced on an Illumina HiSeq X platform (Macrogen Japan, Tokyo, Japan) to obtain 2×150 bp paired-end reads.

### 2.2 | SNP Calling and Filtering

The obtained reads were initially trimmed to remove low-quality sequences and adapters. Trimmed reads were mapped to the reference genome of *Ursus thibetanus japonicus* (GCA\_014364545.1). Variant sites were identified from the resulting BAM files and stored in a single VCF file. These procedures were carried out using the dDocent v2.7.8 pipeline (Puritz et al. 2014).

Variant sites were filtered using VCFtools v0.1.13 (Danecek et al. 2011) in accordance with the SNP Filtering Tutorial (<http://www.ddocent.com/filtering/>). Sites with >50% missing data, minor allele count <3, or quality score <30 were excluded. Samples with >60% missing data were also excluded after treating genotypes with fewer than 3 reads as missing. For the remaining 83 (originally 85) samples, further filtering was applied: mean read depth  $\geq 15$ ,  $\leq 40\%$  missing data, and minor allele frequency  $\geq 0.05$ . Sites deviating from Hardy-Weinberg equilibrium ( $p < 0.001$ ) in each population were also removed. A final filtering step excluded sites with >30% missing data after treating genotypes with <15 reads as missing, retaining only biallelic sites. Linked sites were pruned using PLINK v1.9 (Purcell et al. 2007) based on  $r^2 > 0.25$  within a 50 kb window and excluding sites with observed heterozygosity  $\geq 0.6$ . In addition, 20 bp sequences (i.e., 41 bp) before and after the sites were extracted and BLAST search of their sequences against the sex chromosomes and mitochondrial DNA in the genome data of *Ursus maritimus* (GCA\_017311325.1) was performed to remove the corresponding sites. As a result, a total of 5684 SNPs were retained.

### 2.3 | Population Structure Analysis

Bayesian clustering was conducted using STRUCTURE v2.3.4 (Pritchard et al. 2000). Genetic clusters ( $K$ ) were set from 1 to 10 to infer genetic relationships among samples. Each  $K$  value was tested with a burn-in of 10,000 steps and 10,000 MCMC iterations under an admixture model with correlated allele frequencies (without LOCPRIOR), repeated 10 times independently. LnP(D) values across  $K$  were visualized using CLUMPAK (Kopelman et al. 2015).

To explore the basic genetic distribution among samples, principal coordinate analysis (PCoA) was performed using a genetic distance matrix with imputed missing data. Genetic differentiation among populations was assessed using pairwise  $F_{ST}$  values. Statistical significance of  $F_{ST}$  values was tested by permutation (9999 replicates). Both PCoA and  $F_{ST}$  analyses were performed using GenAlEx 6.503 (Peakall and Smouse 2012). The pairwise  $F_{ST}$  based on mtDNA was also calculated using data from Ohnishi et al. (2009) using Arlequin 3.5.2.2 (Excoffier et al. 2005). To compare genetic diversity among populations, heterozygosity within individuals was calculated using GenAlEx 6.503 software (Peakall and Smouse 2012).

### 2.4 | Demographic History

Historical changes in effective population size ( $Ne$ ) based on nuclear genome data were estimated using Stairway Plot v2.1 (Liu and Fu 2020). The folded 1D-SFS was generated using the python script easySFS (<https://github.com/isaacovercast/easySFS>) based on posterior probabilities of allele frequencies.

Since missing data is common in such datasets, easySFS recommends balancing the number of projected samples and segregating sites (Gutenkunst et al. 2009). Following the heuristic approach of Gutenkunst et al. (2009), projection values that maximized the number of segregating sites were chosen, even if this reduced the number of samples. For each population, 67% of all sites were randomly selected for training. The number of random control points (nrand) for each test was set according to the number of individuals in each population. These breakpoints were treated as points of temporal change in  $Ne$ . Generation time and mutation rate were set at 11.35 years and  $1.83 \times 10^{-8}$  per site per generation (Liu et al. 2014), respectively.

## 3 | Results

### 3.1 | Sequencing Output and SNP Summary

The average number of reads per sample was 2×4,033,440 reads ( $\pm SD$  3,219,623, range: 2×1,515,669 to 2×18,414,561). After filtering, 83 of the original 85 samples were retained for downstream analyses. After removing sites located on sex chromosomes, 5684 SNPs remained for population structure and demographic analyses.

### 3.2 | Genetic Structure

STRUCTURE analysis revealed peaks in  $\Delta K$  at  $K=2$ , 4, and 7 (Figure S1). At  $K=2$ , individuals were divided into two major clusters corresponding to northern Japan and central and western Japan (Figure S2). At  $K=4$ , the northern region was further split into two local populations: Kitakami Mountains (KIT) and Ouu Mountains (OUU), and the Western Chugoku (WCH) population formed a distinct cluster in the west. In contrast, the Central Honshu region remained as a single cluster and was not further subdivided. At  $K=7$ ,  $\Delta K$  showed the second highest value—more than twice that observed at  $K=4$ —and the mean  $\text{LnP}(K)$  plateaued, indicating that  $K=7$  represents a stable and informative clustering level. The bar plots also showed clearly differentiated clusters at this level (Figure 2 and Figure S2). Therefore, subsequent analyses were conducted primarily based on  $K=7$ . When  $K=7$ , two of the five individuals in the Hokuriku population (HOK) showed assignment probabilities below 63%, suggesting genetic affinities with neighboring local populations—Southern Alps (SAL), Eastern–Northern Kinki (ENK), and Kii Peninsula (KII). These three local populations,

together with HOK, constituted the Central Honshu cluster at  $K=4$ .

Principal Coordinate Analysis (PCoA) also revealed regional genetic structure (Figure 3). Populations located at the range periphery—KIT, OUU, and WCH—were clearly separated from the other four populations. Notably, KIT and OUU were widely separated despite their geographical proximity. At  $K=4$  in the STRUCTURE analysis, the Central Honshu cluster was located in the lower left quadrant of the PCoA plot. Among these, SAL, HOK, and KII were positioned close to one another, whereas ENK, despite being geographically adjacent to HOK, was located somewhat apart from the other three local populations.

Pairwise  $F_{ST}$  values between populations are shown in Table 1. The lowest value was observed between HOK and SAL (0.047), followed by HOK and ENK, both of which exhibited relatively low  $F_{ST}$  values. No significant genetic differentiation was found for this pair. The northeastern KIT population showed  $F_{ST}$  values exceeding 0.2 with all other populations, including a value of 0.205 with adjacent OUU. The largest value was observed

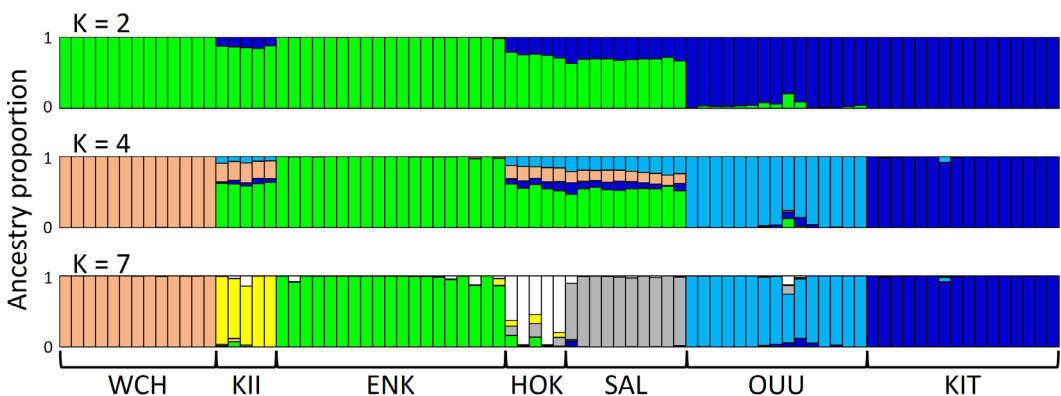


**FIGURE 2** | STRUCTURE analysis results at  $K=2$ , 4, and 7. Local population names are indicated by the labels below. Individuals are arranged from east to west (right to left), except for samples from the KII population, which are placed between ENK and WCH for visual clarity. Vertical axis indicates the proportion of genome assigned to cluster (0–1). See Figure 1 for the abbreviations of local populations.

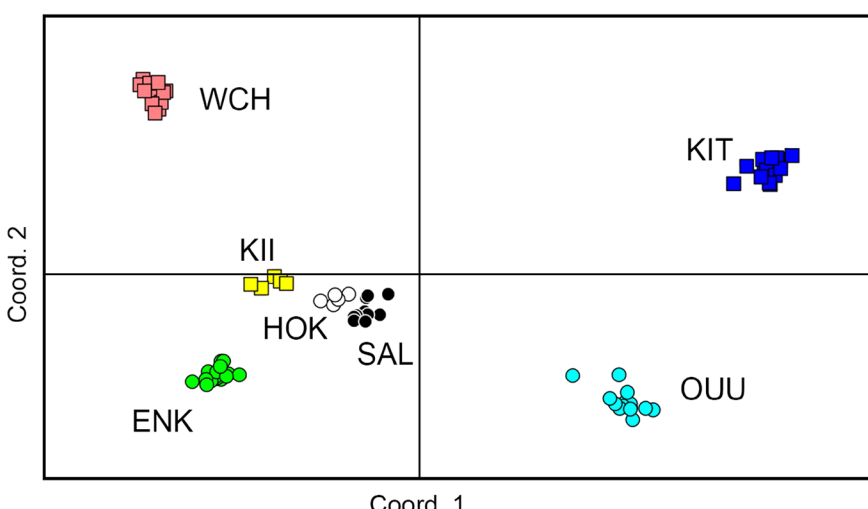


**FIGURE 3** | Results of principal coordinate analysis (PCoA) based on a distance matrix with imputed missing data. Local population names are shown in the figure. See Figure 1 for the abbreviations of local populations.

**TABLE 1** | Genetic distances ( $F_{ST}$ ) among populations of the Asian black bear in Japan.

	<b>KIT</b>	<b>OUU</b>	<b>SAL</b>	<b>HOK</b>	<b>ENK</b>	<b>KII</b>	<b>WCH</b>
KIT		0.543	0.652	0.361	0.887	0.921	0.820
OUU	0.205		0.538	0.178	0.856	0.891	0.787
SAL	0.218	0.164		0.417	0.770	0.823	0.761
HOK	0.212	0.152	0.047*		0.733	0.767	0.642
ENK	0.235	0.186	0.109	0.072**		0.896	0.736
KII	0.286	0.216	0.141	0.103**	0.126		0.820
WCH	0.316	0.272	0.179	0.173	0.194	0.238	

Note: The lower left shows values calculated from Double digest restriction-site associated DNA sequencing (ddRADseq) data in this study. The upper right shows values based on mtDNA analysis, calculated using data published in Ohnishi et al. (2009). The HOK population in the mitochondrial DNA data corresponds to the H and I populations in the study by Ohnishi et al. (2009). See Figure 1 for the abbreviations of local populations.

\* $p=0.011$ .

\*\* $p=0.001$ . All other pairwise comparisons showed  $p < 0.001$ .

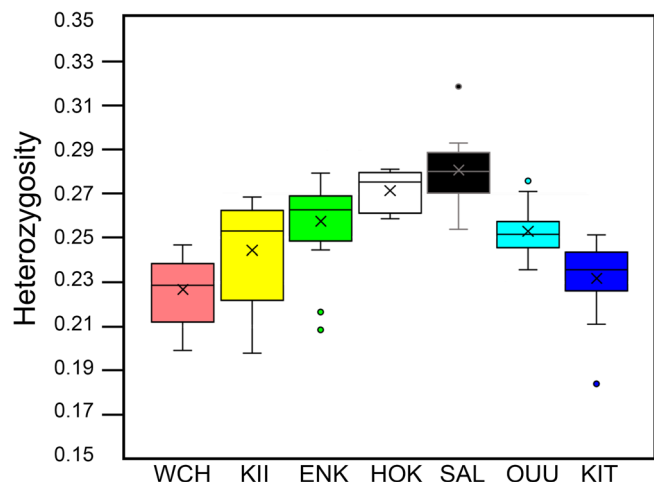


**FIGURE 4** | Intra-individual heterozygosity values for seven populations of Japanese black bears. Boxes represent interquartile ranges; whiskers indicate 1.5 times the interquartile range. The central line and cross in each box represent the median and mean, respectively. Dots indicate individual values that fall outside the whisker range. See Figure 1 for the abbreviations of local populations.

between KIT and WCH (0.316), the two most geographically distant populations. Among the five central and western populations, only the KII-WCH pair had an  $F_{ST}$  exceeding 0.2.

Figure 4 shows individual heterozygosity within each population. The lowest heterozygosity was observed in an individual from KIT (0.184), and the highest in an individual from SAL (0.319). At the population level, SAL had the highest mean heterozygosity, with heterozygosity declining progressively toward both the eastern and western extremes of the distribution. Consistently, the Central Honshu cluster also exhibited high heterozygosity when the number of clusters was set to  $K=4$  (Figure S3).

### 3.3 | Changes in Effective Population Size ( $N_e$ )

Based on the STRUCTURE analysis at  $K=7$ , changes in  $N_e$  were analyzed for each local population (Figure 5). All populations

exhibited a substantial decline in  $N_e$  until approximately 200,000 years ago. The KII population remained stable thereafter, whereas the other populations experienced two additional periods of sharp  $N_e$  decline. HOK showed stabilization around 25,000 years ago, while the remaining five populations continued a gradual decrease after three major declines, persisting until the last few thousand years. When populations were grouped according to the  $K=2$  STRUCTURE clustering (Figure S4), the timing of the initial  $N_e$  decline differed between the Eastern Japan cluster (KIT and OUU) and the Central–Western Japan cluster (SAL, HOK, ENK, KII, and WCH). The eastern cluster began to decline earlier, whereas the western cluster declined at approximately the same time as the pooled dataset including all samples. Under the  $K=4$  clustering, the Central Honshu group (SAL, HOK, ENK, and KII) also began to decline at the same time as the pooled dataset. In contrast, the three remaining local populations—KIT, OUU, and WCH—began to decline earlier. Notably, Central Honshu showed only two major episodes of population decline.

## 4 | Discussion

### 4.1 | Demographic History of Asian Black Bears in Japan

We analyzed changes in effective population size ( $N_e$ ) for seven regional groups identified via STRUCTURE analysis. The results indicated three distinct periods of population decline. The first decline began approximately between 800,000 and 300,000 years ago; the second occurred around 150,000 to 70,000 years ago; and the third from roughly 50,000 to 18,000 years ago. Variation in timing among populations is likely due to error caused by limited sample sizes and a relatively small number of SNPs. It has been suggested that accurate  $N_e$  estimates using ddRADseq require more than 15 samples and over 25,000 SNPs per region (Nunziata and Weisrock 2018). In this study, only three of the seven populations exceeded 15 samples, and the total number of SNPs was limited to 5684, likely affecting the precision of  $N_e$  estimation. In particular, the KII and HOK populations showed little evidence of the second and third population declines, likely due to low detection power, as only five samples were analyzed

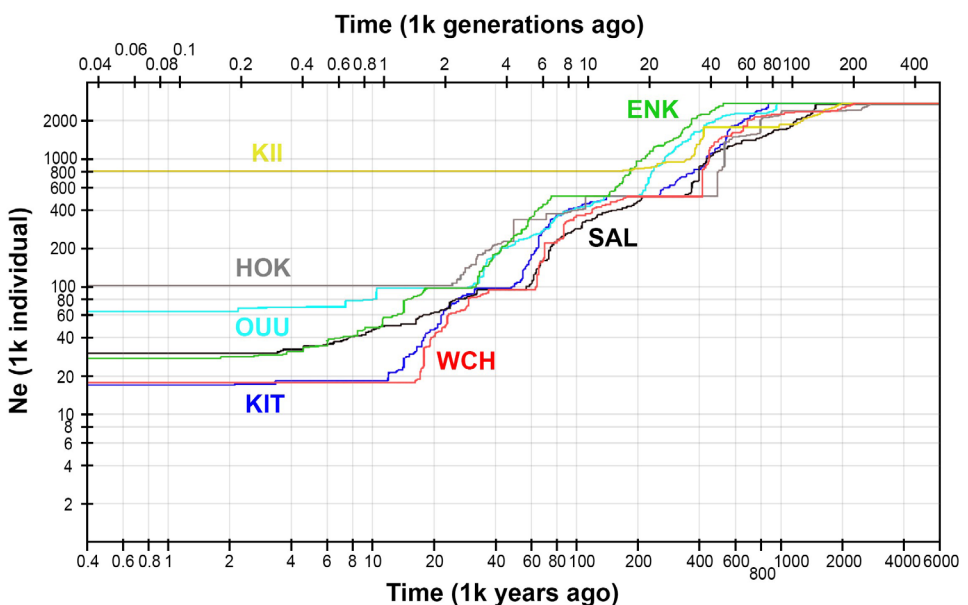


**FIGURE 5** | Changes in effective population size of the seven populations of Asian black bears in Japan identified by STRUCTURE analysis ( $K=7$ ). Local population names are shown in the figure. See Figure 1 for the abbreviations of local populations.

for each. In contrast, KIT, OUU, and WCH populations—with more than 15 samples—experienced a third major decline, followed by a continued gradual decrease that persisted until approximately 2000–3000 years ago. None of the five populations that experienced all three declines showed any sign of  $Ne$  recovery. Despite limited accuracy for each region, consistent trends across populations with more than 10 samples suggest a reliable overall pattern.

Whole-genome sequencing (WGS) data previously reported three episodes of  $Ne$  expansion and contraction, with  $Ne$  peaks observed around 700,000, 30,000, and 1000 years ago (Kishida et al. 2022). In contrast, the present ddRADseq data captured only the three declines in  $Ne$  and not the increases. These declines likely correspond to post-peak periods reported in the WGS study. The first decline may be associated with the arrival of Asian black bears in Japan from the Asian continent. Mitochondrial genome-based demographic reconstructions have shown that continental populations expanded around 400,000 years ago and declined sharply after 20,000 years ago (Kumar et al. 2017). Whole-genome sequencing data of two Japanese individuals presented by Kishida et al. (2022) showed a sharp population expansion approximately 70,000 years ago, followed by a major decline. While differences in assumptions regarding generation time ( $g$ ) and mutation rate ( $\mu$ ) prevent direct comparisons, continental populations appear to have maintained relatively stable numbers after moderate declines, whereas Japanese populations experienced more dramatic reductions. This supports the hypothesis that the migration to Japan occurred shortly after the mid-Pleistocene expansion on the continent.

The second  $Ne$  reduction may reflect habitat loss triggered by the onset of the Last Glacial Period, which began around 70,000 years ago. During the LGM, broadleaf forests in high-elevation areas and northeastern Japan were replaced by coniferous forests, and black bears were likely restricted to lowland

refugia (Ohnishi et al. 2009). Although sea levels dropped and land emerged in areas such as the Seto Inland Sea, connecting Honshu, Shikoku, and Kyushu, these areas were likely wetlands, limiting bear range expansion (Yamaguchi et al. 2014).

The third decline corresponds to the timing of the  $Ne$  peak followed by a decline observed in the WGS-based analysis by Kishida et al. (2022), which occurred around 30,000 years ago. In this study, the same values for generation time and mutation rate as used by Kishida et al. were adopted, allowing for direct comparison. This decline may be related to human expansion. Humans are believed to have arrived in Japan as early as 38,000 years ago (Nakazawa 2017), and Y-chromosome genome analysis suggests a human population increase began around 12,500 years ago (Watanabe et al. 2019). The continued gradual decline in  $Ne$  observed in the present study following the third major reduction—persisting until approximately 2000–3000 years ago—may also be related to this demographic expansion. Although the accuracy of the present data is limited, the observed  $Ne$  trends are consistent with these historical events.

Although Stairway Plot 2 is considered more suitable than SMC-based methodologies such as PSMC for detecting very recent changes in effective population size—its advantage being limited to the past ~16 generations (approximately 200 years ago to the present), whereas PSMC provides more reliable inference for demographic changes prior to ~3000 years ago (Patton et al. 2019), the resolution of the present results was lower than that of the PSMC-based analysis by Kishida et al. (2022). Because the present study focuses primarily on population fluctuations that occurred more than 2000–3000 years ago, PSMC is in fact the more appropriate framework for resolving demographic history within this timescale. As discussed above, this is likely due to the limited number of samples and SNPs available in the current dataset.

## 4.2 | Population Structure of Asian Black Bears

Bayesian clustering clearly revealed a distinct population structure. This result aligns with previous microsatellite-based studies in northern Japan, particularly around the OUU population, which also detected clear genetic clusters.

Genetic diversity was highest in SAL, located in the central part of the distribution, followed by HOK and ENK. In contrast, peripheral populations such as KIT and WCH showed the lowest diversity among the seven groups analyzed. This high diversity in SAL was also reported in mtDNA analyses. According to Ohnishi et al. (2009), who analyzed gene diversity ( $H$ ) based on the mitochondrial DNA control region, SAL exhibited the highest value ( $H=0.78$ ) among the same seven local populations, followed by HOK (0.74; groups *H* and *I* in that study), while the remaining five populations all had  $H$  below 0.50.

The high diversity in SAL is likely due to its habitat environment—dominated by deciduous and evergreen broadleaf forests—favorable for black bears both in the past and at present. Although high-elevation habitats were likely lost during the LGM, lowland coastal areas on the southern side are believed to have remained covered by broadleaf forests even during glacial maxima (Okaura and Harada 2002), allowing large populations to persist. Furthermore, the region also includes the deep, mountainous South Alps, characterized by low human population density and stable bear populations at present.

The current findings are well-suited for examining sex-biased dispersal in Asian black bears. The Bayesian analysis suggested that the HOK population has received gene flow from three adjacent populations. It was genetically closest to SAL in the principal coordinate analysis and showed no significant  $F_{ST}$  difference from SAL.

However, mtDNA-based analysis showed higher  $F_{ST}$  values between HOK and SAL (0.417), ENK (0.733), and KII (0.767). Previous phylogeographic studies using mtDNA identified three major lineages in Japan, separated by Lake Biwa. In our study, HOK grouped with KIT and OUU in the northern cluster, ENK and WCH in the western cluster, and KII in the southern cluster. While mtDNA reflects strong female philopatry, nuclear genome data revealed gene flow across mtDNA-defined cluster boundaries—likely due to male-mediated natal dispersal.

Population continuity also affects gene flow. Landscape genetic analyses around the OUU region in northern Japan showed that agricultural and residential areas acted as 25-fold stronger resistance to gene flow (Ohnishi et al. 2009). In regions west of ENK, including WCH, three isolated populations exist. Microsatellite analysis comparing these to the eastern continuous populations revealed an  $F_{ST}$  of 0.078 between eastern HOK and ENK, comparable to the  $F_{ST}$  found in this study, supporting the role of continuity in maintaining gene flow. Similarly, WCH exhibited  $F_{ST}$  values  $\geq 0.173$  with all other populations, and KIT showed an  $F_{ST}$  of 0.205 even with neighboring OUU.

All three isolated populations—KIT, WCH, and KII—had low heterozygosity. Although Figure 5 might suggest a correlation

between peripheral distribution and reduced diversity, this pattern is likely due to limited gene flow from isolation and genetic drift from population declines. Phylogeographic mtDNA studies suggest that in northern Japan, small refugial populations during the LGM reduced diversity, whereas in western Japan (including KII and WCH), human activities such as deforestation and hunting over the past 200–300 years led to population decline (Ohnishi et al. 2009). Interestingly, despite its isolation, the KII population showed signs of gene flow with HOK, and  $F_{ST}$  values below 0.15 with ENK and SAL. Given its geographical proximity to these continuous populations, gene flow likely persisted until relatively recently. In addition, compared to KIT and WCH, the Kii Peninsula, where KII is located, is characterized by a relatively warm climate, which may have allowed the persistence of a larger population even during the Last Glacial Maximum (LGM). Phylogeographic studies have suggested that refugia of deciduous broadleaf species, such as *Quercus mongolica* var. *crispula* (Okaura and Harada 2002), were present in the Kii Peninsula during the LGM, implying that suitable habitats for black bears may also have persisted there. This could have contributed to the retention of higher genetic diversity in KII.

## 4.3 | Concluding Remarks

This study conducted a reduced-representation genome analysis using multiple samples from several local populations of Asian black bears in Japan. It represents the first wide-ranging genomic study on this species, aiming to capture the historical dynamics of peripheral island populations. Although the sampling did not cover the entire distribution range, it included three isolated populations at the range periphery, two populations at the northern and southern ends of a large continuous population (OUU and ENK), and two populations (HOK and SAL) likely representing the core of this continuous range. This well-balanced design provides sufficient resolution to outline the demographic and genetic history of Japanese black bears in Honshu. We successfully detected three population declines, although resolution was lower than that of WGS-based studies. We are currently conducting WGS analyses with additional samples to clarify regional patterns of demographic change and elucidate the distribution history of island populations in the Far East. Our analysis of population structure revealed clear signals of local population units, uncovering differences in male and female dispersal patterns that were not evident from mtDNA analyses alone. It also highlighted unique features of isolated populations at the range periphery. However, it is regrettable that we were unable to include the Shikoku population, which is both phylogenetically distinct based on mitochondrial DNA and currently facing a high risk of extinction. Tissue samples from Shikoku with sufficient quality and quantity for ddRAD-seq were not available for this study. Including this critically endangered population in future genomic analyses remains an important research priority. Future research should focus on a broader-scale investigation of the continuous populations in eastern Japan as well as genomic assessments of understudied or endangered local populations such as that of Shikoku, to support long-term conservation strategies.

## Acknowledgments

We thank the prefectural government offices and local hunting associations of Iwate, Shizuoka, Ishikawa, Fukui, Shiga, Kyoto, Mie, and Shimane for providing samples. We also express our sincere gratitude and remembrance to the late Yasuko Segawa, who supported sample curation. This work was supported by JSPS KAKENHI Grant Number 22H02370 and 25K02037, the Environment Research and Technology Development Fund (JPMEERF20254002) of the Environmental Restoration and Conservation Agency provided by Ministry of the Environment of Japan, the research support by Mountain Science Center, University of Tsukuba and the Support program of FFPRI for researchers having family obligations. A part of this study was carried out within the state assignment of Ministry of Science and Higher Education of the Russian Federation (theme No. 124012200182-1). Valentin Guskov was supported by the Japan–Russia Youth Exchange Center (JREX) during his research stay in Japan.

## Funding

This work was supported by the Support program of FFPRI for researchers having family obligations, the Japan Society for the Promotion of Science (22H02370, 25K02037), the Ministry of Science and Higher Education of the Russian Federation (124012200182-1), the Mountain Science Center, University of Tsukuba and the Environment Research and Technology Development Fund (JPMEERF20254002).

## Conflicts of Interest

The authors declare no conflicts of interest.

## References

Cronin, M. A. 1993. "In My Experience: Mitochondrial DNA in Wildlife Taxonomy and Conservation Biology: Cautionary Notes." *Wildlife Society Bulletin (1973–2006)* 21: 339–348.

Danecek, P., A. Auton, G. Abecasis, et al. 2011. "The Variant Call Format and VCFtools." *Bioinformatics* 27, no. 15: 2156–2158.

De Kort, S. R., C. P. Pinheiro, and C. Vieira. 2021. "Genetic Structure and Phylogeography of Three Co-Distributed Small Mammals in the Atlantic Forest." *Journal of Biogeography* 48, no. 5: 1123–1136.

Edwards, S., and S. Bensch. 2009. "Looking Forwards or Looking Backwards in Avian Phylogeography. A Comment on Zink and Barrowclough 2008." *Molecular Ecology* 18: 2930–2933.

Excoffier, L., G. Laval, and S. Schneider. 2005. "Arlequin ver. 3.0: An Integrated Software Package for Population Genetics Data Analysis." *Evolutionary Bioinformatics Online* 1: 47–50.

Groom, M. J., Y. S. Chyi, and C. R. Carroll. 2006. *Principles of Conservation Biology*. Sinauer.

Gutenkunst, R. N., R. D. Hernandez, S. H. Williamson, and C. D. Bustamante. 2009. "Inferring the Joint Demographic History of Multiple Populations From Multidimensional SNP Frequency Data." *PLoS Genetics* 5, no. 10: e1000695. <https://doi.org/10.1371/journal.pgen.1000695>.

Hohenlohe, P. A., W. C. Funk, and O. P. Rajora. 2021. "Population Genomics for Wildlife Conservation and Management." *Molecular Ecology* 30, no. 1: 62–82. <https://doi.org/10.1111/mec.15720>.

Kawamura, Y. 2000. "Immigration of Mammals Into Japan During the Quaternary, With Comments on Land or Ice Bridge Formation Enabled Human Immigration." *Acta Anthropologica Sinica* 19: 264–269.

Kishida, T., M. Ohashi, and Y. Komatsu. 2022. "Genetic Diversity and Population History of the Japanese Black Bear (*Ursus thibetanus japonicus*) Based on the Genome-Wide Analyses." *Ecological Research* 37, no. 5: 647–657. <https://doi.org/10.1111/1440-1703.12335>.

Kopelman, N. M., J. Mayzel, M. Jakobsson, N. A. Rosenberg, and I. Mayrose. 2015. "Clumpak: A Program for Identifying Clustering Modes and Packaging Population Structure Inferences Across K." *Molecular Ecology Resources* 15: 1179–1191.

Kumar, V., F. Lammers, T. Bidon, et al. 2017. "The Evolutionary History of Bears Is Characterized by Gene Flow Across Species." *Scientific Reports* 7: 46487. <https://doi.org/10.1038/srep46487>.

Liu, S., E. D. Lorenzen, M. Fumagalli, et al. 2014. "Population Genomics Reveal Recent Speciation and Rapid Evolutionary Adaptation in Polar Bears." *Cell* 157: 785–794. <https://doi.org/10.1016/j.cell.2014.03.054>.

Liu, X., and Y. X. Fu. 2020. "Stairway Plot 2: Demographic History Inference With Folded SNP Frequency Spectra." *Genome Biology* 21: 280. <https://doi.org/10.1186/s13059-020-02196-9>.

Meffe, G. K., and C. R. Carroll. 1997. *Principles of Conservation Biology*. Sinauer.

Nakazawa, Y. 2017. "On the Pleistocene Population History in the Japanese Archipelago." *Current Anthropology* 58, no. S17: S539–S552. <https://doi.org/10.1086/694447>.

Nunziata, S. O., and D. W. Weisrock. 2018. "Estimation of Contemporary Effective Population Size and Population Declines Using RAD Sequence Data." *Heredity* 120, no. 3: 196–207. <https://doi.org/10.1038/s41437-017-0037-y>.

Ohnishi, N., and T. Osawa. 2014. "A Difference in the Genetic Distribution Pattern Between the Sexes in the Asian Black Bear." *Mammal Study* 39, no. 1: 11–16.

Ohnishi, N., R. Uno, Y. Ishibashi, H. B. Tamate, and T. Oi. 2009. "The Influence of Climatic Oscillations During the Quaternary Era on the Genetic Structure of Asian Black Bears in Japan." *Heredity* 102, no. 6: 579–589.

Okaura, T., and K. Harada. 2002. "Genetic Structure and Phylogeography of Japanese Beech (*Fagus Crenata* Blume) Based on Chloroplast DNA Variation." *Heredity* 88, no. 4: 322–329.

Patton, A. H., M. J. Margres, A. R. Stahlke, et al. 2019. "Contemporary Demographic Reconstruction Methods Are Robust to Genome Assembly Quality: A Case Study in Tasmanian Devils." *Molecular Biology and Evolution* 36, no. 12: 2906–2921.

Peakall, R., and P. E. Smouse. 2012. "GenAlEx 6.5: Genetic Analysis in Excel. Population Genetic Software for Teaching and Research: An Update." *Bioinformatics* 28: 2537–2539.

Peterson, B. K., J. N. Weber, E. H. Kay, H. S. Fisher, and H. E. Hoekstra. 2012. "Double Digest RADseq: An Inexpensive Method for de Novo SNP Discovery and Genotyping in Model and Non-Model Species." *PLoS One* 7, no. 5: e37135.

Pritchard, J. K., M. Stephens, and P. Donnelly. 2000. "Inference of Population Structure Using Multilocus Genotype Data." *Genetics* 155, no. 2: 945–959.

Purcell, S., B. Neale, K. Todd-Brown, et al. 2007. "PLINK: A Tool Set for Whole-Genome Association and Population-Based Linkage Analyses." *American Journal of Human Genetics* 81, no. 3: 559–575.

Puritz, J. B., C. M. Hollenbeck, and J. R. Gold. 2014. "dDocent: A RADseq, Variant-Calling Pipeline Designed for Population Genomics of Non-Model Organisms." *PeerJ* 2: e431.

Takayama, K., N. Ohnishi, A. Zedrosser, et al. 2023. "Timing and Distance of Natal Dispersal in Asian Black Bears." *Journal of Mammalogy* 104, no. 2: 265–278. <https://doi.org/10.1093/jmammal/gyacl18>.

Toews, D. P. L., and A. Brelsford. 2012. "The Biogeography of Mitochondrial and Nuclear Discordance in Animals." *Molecular Ecology* 21, no. 16: 3907–3930.

Watanabe, Y., I. Naka, S.-S. Khor, et al. 2019. "Analysis of Whole Y-Chromosome Sequences Reveals the Japanese Population History in the Jomon Period." *Scientific Reports* 9, no. 1: 8556. <https://doi.org/10.1038/s41598-019-44473-z>.

Wu, J., N. Kohno, S. Mano, et al. 2015. "Phylogeographic and Demographic Analysis of the Asian Black Bear (*Ursus thibetanus*) Based on Mitochondrial DNA." *PLoS One* 10, no. 9: e0136398. <https://doi.org/10.1371/journal.pone.0136398>.

Yamaguchi, K., T. Takeuchi, S. Onodera, and K. Kitaoka. 2014. "Formation Process of the Holocene Clay Layer in a Coastal Alluvial Plain of an Enclosed Sea: Case Study of the Okayama Plain." *Journal of Japanese Association of Hydrological Sciences* 44, no. 3: 161–177.

## Supporting Information

Additional supporting information can be found online in the Supporting Information section. **Figure S1:** Mean posterior probability ( $\text{LnP}(D)$ ) values (a) and the delta  $K$  value (b) from  $K=1$  to  $K=10$ . Vertical bars around  $\text{LnP}(D)$  represent standard deviations across replicate runs. **Figure S2:** Results of STRUCTURE analysis at  $K=1$  to 10. Regional population names are indicated by the labels below. Individuals are arranged from east to west (right to left), except for samples from the KII population, which are placed between ENK and WCH for visual clarity. Vertical axis indicates the proportion of genome assigned to cluster (0–1). See Figure 1 for the abbreviations of local populations. **Figure S3:** Heterozygosity values in four populations of the Asian black bear in Japan, as defined by the STRUCTURE analysis at  $K=4$ , with Central Honshu comprising SAL, HOK, ENK, and KII. Boxes represent interquartile ranges; whiskers indicate 1.5 times the interquartile range. The central line and cross in each box represent the median and mean, respectively. Dots indicate individual values that fall outside the whisker range. See Figure 1 for the abbreviations of local populations. **Figure S4:** Demographic trajectories of Asian black bear populations in Japan as inferred using Stairway Plot 2. Effective population size ( $N_e$ ) is plotted on a log scale on the y-axis, and time before present (in thousands of years or generations) is shown on the x-axis. The top panel shows three pooled population groups: all individuals (green), the Central and Western Honshu cluster (SAL, HOK, ENK, KII, and WCH; red), and the Northern Honshu cluster (KIT and OUU; blue) identified at  $K=2$  in the STRUCTURE analysis. The bottom panel shows demographic histories of individual local populations identified under  $K=4$  in the STRUCTURE analysis: Central Honshu (SAL, HOK, ENK, and KII; green), OUU (cyan), WCH (red), and KIT (blue). See Figure 1 for the abbreviations of local populations. **Table S1:** Genetic distances (FST) among four populations of the Asian black bear in Japan. These four populations correspond to those identified when  $K=4$  in the STRUCTURE analysis, with Central Honshu comprising SAL, HOK, ENK, and KII. See Figure 1 for the abbreviations of local populations.